

See discussions, stats, and author profiles for this publication at: <https://www.researchgate.net/publication/231238053>

Nanopatterned Magnetic Metal via Colloidal Lithography with Reactive Ion Etching

ARTICLE in CHEMISTRY OF MATERIALS · SEPTEMBER 2004

Impact Factor: 8.35 · DOI: 10.1021/cm048688s

CITATIONS

39

READS

14

6 AUTHORS, INCLUDING:



Dae-Geun Choi

Korea Institute of Machinery and Materials

106 PUBLICATIONS 1,788 CITATIONS

SEE PROFILE



Se Gyu Jang

Korea Institute of Science and Technology

54 PUBLICATIONS 1,481 CITATIONS

SEE PROFILE



Jong-Ryul Jeong

Chungnam National University

90 PUBLICATIONS 1,099 CITATIONS

SEE PROFILE



Sung Chul Shin

Gyeongsang National University

268 PUBLICATIONS 3,032 CITATIONS

SEE PROFILE

Nanopatterned Magnetic Metal via Colloidal Lithography with Reactive Ion Etching

Dae-Geun Choi,^{†,§} Sarah Kim,[†] Se-Gyu Jang,[†]
Seung-Man Yang,^{*,†} Jong-Ryul Jeong,[‡] and
Sung-Chul Shin[‡]

Department of Chemical and Biomolecular
Engineering and Department of Physics & Center for
Nanospinics of Spintronic Materials, Korea Advanced
Institute of Science and Technology,
373-1 Guseong-dong, Yuseong-gu,
Daejeon 305-701, Korea

Received August 9, 2004

Revised Manuscript Received September 11, 2004

Two-dimensional patterned surfaces have attracted great attention because of their potential uses in biochips and sensors,¹ electronic devices,² magnetic recording devices,³ photonic crystals,⁴ and templates for novel materials.⁵ Various nanofabrication techniques have been used to construct such patterned surfaces, including soft lithography⁶ and laser interference lithography.⁷ Several self-assembly techniques employing block copolymers⁸ and colloidal particles have also been used to create 2D patterns.⁹ Specifically, well-organized 2D particle arrays are of practical significance for applications in soft lithography,¹⁰ microlenses,¹¹ carbon nanotube arrays,¹² and colloidal lithography (CL). In CL, colloidal arrays are used as lithographic masks or templates to fabricate nanostructures.¹³ CL has several advantages: it is an inexpensive, inherently parallel, high-throughput nanofabrication technique.¹³ Primarily, single and double layers of colloidal particles have been used in CL as templates for patterned polymers and metals. In general, interstices between the particles

were used for infiltration of the polymers and metals. A close-packed colloidal assembly usually forms interstices with hexagonal shapes in a single layer or triangular shapes in a double layer.

However, the use of CL with a self-organized particle array entails a difficulty in controlling the size and shape of a structure. Generally, the size and shape of a final nanostructure are dependent on the original colloidal template. Recently, several techniques to control the size and shape of nanostructures have been suggested, including angle-resolved deposition¹⁴ and control of deposition thickness and dry-etching conditions.¹⁵ These methods have utilized the interstices of the *close-packed* colloidal layer to control nanostructure size and shape. In these methods, however, the feature size and shape were determined from the original nanostructure of colloidal arrays and could not be changed for a given colloidal layer. Thus, controlling nanostructures is still a challenging issue, and new techniques are needed.

This paper describes a novel method for the fabrication of patterned arrays of Co/Pt multilayer by using the CL technique in combination with the reactive ion etching (RIE) method that has been developed recently in our group to control the colloidal nanopatterns with RIE.^{16a} Specifically, we extend here our previous study to pattern transfer for magnetic devices. In CL, a patterned layer of monodisperse colloidal spheres was used as a mask for the deposition or etching of the magnetic Co/Pt multilayer. Among the important features of the present method is that the size, shape, and feature spacing of the magnetic metal dot arrays were controlled simply by changing the conditions of the precedent RIE of the colloidal mask layer such as the etching time, etchant composition, and tilt angle. This is of practical significance in magnetic memory devices because the magnetic properties of metal dots are sensitive to particle size and shape. Specifically, we created the magnetic metal patterns with controllable features such as circular and triangular dots or holes using the RIE-assisted colloidal masks of single-layered or double-layered polystyrene (PS) beads, and analyzed the magnetic properties of the magnetic metal dots by using a magnetooptical microscope magnetometer (MOMM).

Figure 1 shows the experimental scheme. To fabricate patterned magnetic metal dots of Co/Pt multilayer, the wafer substrates were cleaned with piranha solution (3:1 concentrated H₂SO₄/30% H₂O₂), and the substrates were rinsed with deionized water, acetone, and methanol under sonication. Colloidal PS spheres of 200-nm diameter were synthesized by emulsifier-free emulsion polymerization¹⁷ and were dispersed in water and then further diluted in methanol (4 wt %, 2 wt %). We used two different strategies: in strategy I of Figure 1a, we began with the deposition of 10 layers of Co/Pt

* Corresponding author. E-mail: smyang@kaist.ac.kr.

[†] Department of Chemical and Biomolecular Engineering.

[‡] Department of Physics & Center for Nanospinics of Spintronic Materials.

[§] Present address: Department of Intelligent Precision Machine, Nanomechanisms Group, Korea Institute of Machinery & Materials, 171 Jang-dong, Yuseong-gu, Daejeon, 305-343, Republic of Korea.

(1) Cui, Y.; Wei, Q. Q.; Park, H. K.; Leiber, C. M. *Science* **2001**, 293, 1289.

(2) Xia, Y.; Kim, E.; Zhao, X. M.; Rogers, J. A.; Prentiss, M.; Whitesides, G. M. *Science* **1996**, 273, 347.

(3) (a) Stuart, H. R.; Hall, D. G. *Appl. Phys. Lett.* **1996**, 69, 2327.

(b) Chou, S. Y.; Wei, M. S.; Krauss, P. R.; Fischer, P. B. *J. Appl. Phys.* **1994**, 76, 6673.

(4) Shi, H. Q.; Tsai, W. B.; Garrison, M. D.; Ferrari, S.; Ratner, B. D. *Nature* **1999**, 398, 593.

(5) Jiang, P.; Bertone, J. F.; Colvin, V. L. *Science* **2001**, 291, 453.

(6) Xia, Y. N.; Whitesides, G. M. *Angew. Chem., Int. Ed.* **1998**, 37, 551.

(7) Shoji, S.; Kawata, S. *Appl. Phys. Lett.* **2000**, 76, 2668.

(8) Zhao, D.; Feng, J.; Huo, Q.; Melosh, N.; Fredrickson, G. H.; Chemelka, B. F.; Stucky, G. D. *Science* **1998**, 279, 548.

(9) Chen, X.; Chen, Z.; Fu, N.; Lu, G.; Yang, B. *Adv. Mater.* **2003**, 15, 1413.

(10) (a) Kuo, C.-W.; Shiu, J.-Y.; Cho, Y.-H.; Chen, P. *Adv. Mater.* **2003**, 15, 1065. (b) Choi, D.-G.; Jang, S.-G.; Yu, H. K.; Yang, S.-M. *Chem. Mater.* **2004**, 16, 3410.

(11) Wu, M.-H.; Whitesides, G. M. *Appl. Phys. Lett.* **2001**, 78, 2273.

(12) Hung, Z. P.; Carhahan, D. L.; Rybcynski, J.; Giersig, M.; Sennett, M.; Wang, D. Z.; Wen, J. G.; Kempa, K.; Ren, Z. F. *Appl. Phys. Lett.* **2003**, 82, 460.

(13) (a) Haynes, C. L.; Van Duyne, R. P. *J. Phys. Chem. B* **2001**, 105, 5599. (b) Yi, D. K.; Kim, D.-Y. *Chem. Commun.* **2003**, 982.

(14) Haynes, C. L.; McFarland, A. D.; Smith, M. T.; Hulteen, J. C.; Van Duyne, R. P. *J. Phys. Chem. B* **2002**, 106, 1898.

(15) Kuo, C.-W.; Shiu, J.-Y.; Chen, P. *Chem. Mater.* **2003**, 15, 2917.

(16) (a) Choi, D.-G.; Yu, H. K.; Jang, S. G.; Yang, S.-M. *J. Am. Chem. Soc.* **2004**, 126, 7019. (b) Tada, T.; Hamoudi, A.; Kanayama, T.; Koga, T. K. *Appl. Phys. Lett.* **1997**, 70, 2538.

(17) Yi, G. R.; Moon, J. H.; Yang, S.-M. *Chem. Mater.* **2001**, 13, 2613.

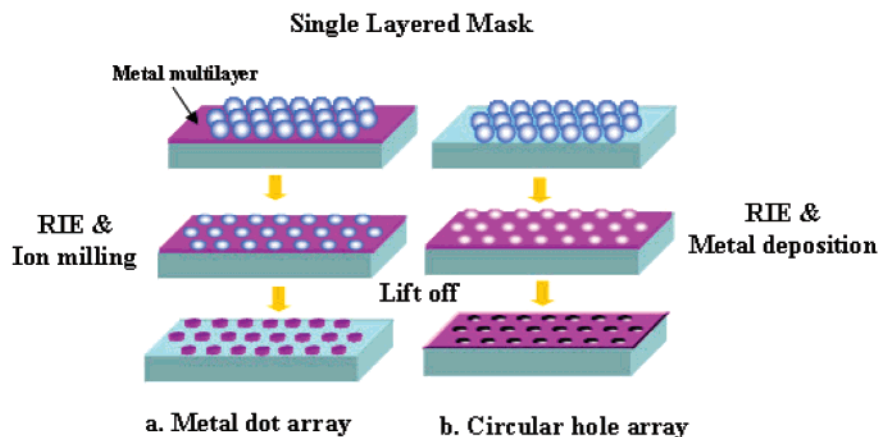


Figure 1. Schematic diagram for experimental process of (a) magnetic metal dot pattern (strategy I) (b) circular hole pattern (strategy II) by using a single-layered colloidal mask.

(4 Å Co/11 Å Pt)₁₀ onto a silicon wafer using a dc magnetron sputtering under a base pressure of 2×10^{-4} mTorr and Ar sputtering pressure of 5 mTorr at an ambient temperature. The deposition rates were 0.5 Å/s for Co and 1.1 Å/s for Pt under an applied power of 30 W to each target. The target-to-substrate distance was kept at 75 mm. The Co/Pt multilayer had strong perpendicular magnetic anisotropy and showed the magnetic hysteresis loop of unit squareness. The Co/Pt film was treated with oxygen plasma for 1 min to make it hydrophilic. Then a colloidal mask was formed by spin-casting the PS bead suspension onto the Co/Pt multilayer film. The number of colloidal layers was adjusted by the spin-coating speed and the PS bead concentration. To modify the shape and feature spacing of the colloidal mask, the RIE was performed directly onto the preformed well-ordered colloidal particle array with a 3:2 mixture of O₂ and CF₄ under 60 mTorr with a power of 60 W. Subsequently, the Ar ion milling was conducted to etch out the Co/Pt layer, which left behind the array of Co/Pt dots where the PS beads shadowed. The DC bias for the ion milling was 400 V and the Ar pressure was kept below 5×10^{-4} Torr. Finally, the PS beads were removed by sonicating the substrate in CH₂Cl₂ solution for 5 min.

In strategy II of Figure 1b, a colloidal mask was formed first onto a wafer, which was followed by the RIE-assisted feature modification. The PS beads were removed by the same method as that used in strategy I. Then the patterns of metal dots were formed by deposition of Co/Pt through the interstices between the PS beads. In both cases, the morphology was observed by SEM (Philips-XL20SFEG) and AFM (SEIKO SPA400).

Figure 2a shows a PS bead array that was obtained by RIE for 60 s on the monolayer of hexagonally close-packed PS spheres that were spin-cast onto the Co/Pt multilayer. Defect-free domains were in the range from several to a few hundred square micrometers (μm^2). The size of the PS beads in Figure 2a is about 145 nm; their original size was 200 nm. The diameter of the PS particles was gradually reduced as the RIE time increased. In our experiment, the particle size was reduced to 45 nm after RIE for 240 s. The use of a gas mixture of O₂/CF₄ resulted in slower etching with better controllability than the use of pure O₂, because O₂ has a greater reactivity with polymer.¹⁶ Figure 2b shows the AFM and SEM images of the Co/Pt metal dot array that

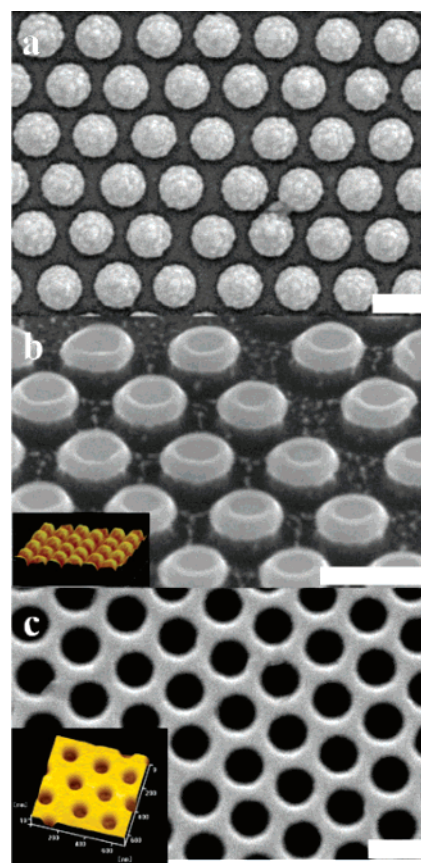


Figure 2. SEM images of (a) single-layered PS arrays after O₂/CF₄ RIE for 60 s. (b) SEM and AFM images of Co/Pt metal dot pattern after removal of the single-layered PS beads by lift-off process. After RIE treatment for 60 s, ion milling for 90 s was performed to etch the magnetic metal layer. SEM image was taken with a tilted angle at 45°. (c) SEM and AFM images of Co/Pt magnetic film with circular hole array. Scale bars are 200 nm.

was left behind after Ar ion milling for 90 s. As noted, a completely isolated metal dot array was formed by strategy I.

To obtain an array of circular holes on the Co/Pt film by following strategy II (Figure 1b), a lift-off process of the colloidal mask was performed after the Co/Pt deposition on the PS monolayer film previously etched by means of RIE. The diameter of the hole in the SEM image of Figure 2c was about 135 nm. The feature

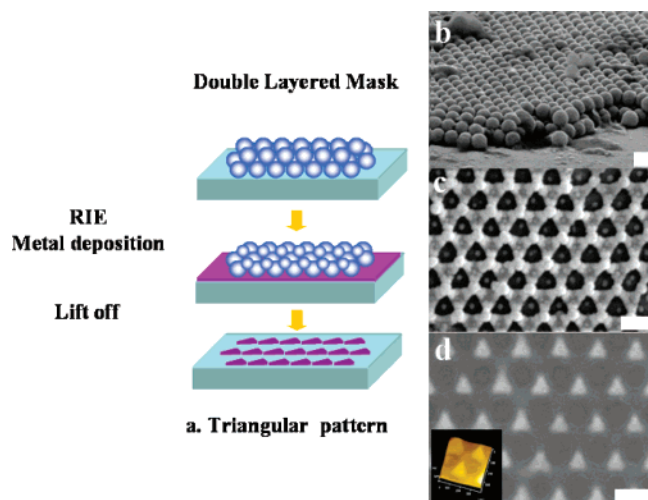


Figure 3. (a) Schematic for the fabrication of triangular metal dot pattern. (b) SEM image of the as-deposited double-layered PS colloidal array prior to RIE. (c) SEM image of the etched PS double layer after RIE for 90 s. (d) SEM and AFM images of triangular Co/Pt metal dot array that was fabricated by the scheme in (a). RIE time was 60 s. Scale bars are 200 nm.

distance of the hole array depended solely on the size of the original PS beads. Meanwhile, the hole size was reduced with the RIE time. The depth of the hole was about 15 nm, as shown in the AFM image of Figure 2c.

As schematically shown in Figure 3a, a patterned array of Co/Pt metal dots in triangular shape was obtained by using a double-layered colloidal PS mask produced from the RIE process, which used a relative shadowing effect.^{16a} The SEM image of the as-deposited double-layered PS colloidal array prior to RIE is shown in Figure 3b. Indeed, due to the relative shadowing effect, the etched PS double layer after RIE for 90 s formed a colloidal mask with triangular pattern, as shown in Figure 3c. The resulting AFM and SEM images of the patterned array of Co/Pt metal dots are shown in Figure 3d. The in-plane diameter of the triangular Co/Pt dots in the SEM image of Figure 3d is about 90–100 nm and the thickness of the dots in the AFM image is about 15 nm.

Due to their high coercivity and strong magnetocrystalline anisotropy, Co/Pt multilayer films have been applied in high-density magnetic recording media and hard magnetic layers in spin valve structures.¹⁸ We investigated the magnetic properties of continuous multilayer Co/Pt film and Co/Pt nanodot array with MOMM. The MOMM system mainly consists of an optical polarizing microscope capable of imaging magnetic domain through the magneto-optical Kerr effect. A charge coupled device (CCD) camera captures the domain image in the form of the array of the Kerr intensity measured from the CCD pixels. By storing the domain images and tracing the Kerr intensity variation for every individual CCD pixel, a minimum area for a proper probe is $400 \times 400 \text{ nm}^2$. In this work, we probed a $10 \times 10 \text{ }\mu\text{m}^2$ area of the sample. Figure 4 shows magnetic hysteresis loops of Co/Pt continuous film and nanodot arrays. The interdot distance of the nanodot

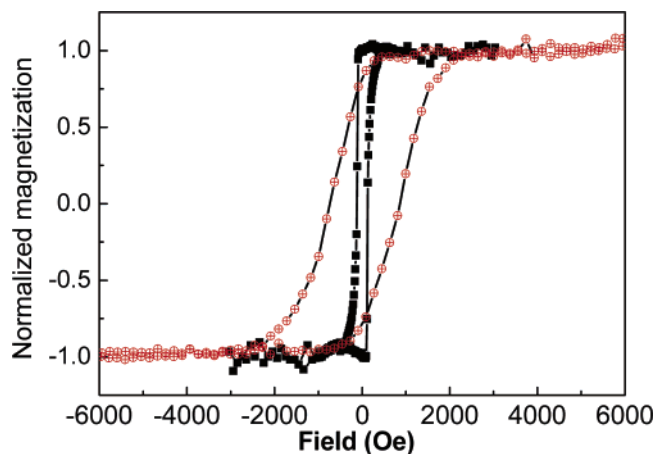


Figure 4. Magnetic hysteresis loops of Co/Pt multilayer film (black square) and Co/Pt multilayer nanodot array with 200-nm interdot distance and 150-nm dot size (open circle).

array is about 200 nm and the dot size is 150 nm diameter. As noted, the patterned nanodots increased the coercivity relative to that of the continuous film. It could be ascribed to the suppression of multidomain formation during magnetization reversal for the patterned nanodots.^{19–22} Also noted is that the loop slope of the nanodot array at the coercive point is decreased compared to that of the continuous film, which implies the enhancement of switching width.

Colloidal self-assembly does not produce defect free areas due to nanosphere polydispersity, site randomness, vacancies, line defects, and polycrystalline domains. Moreover, the magnetic properties of Co/Pt nanodot array strongly depend on geometrical structure, such as dot shape, array structure, defect, and others. Therefore, we have investigated the variation of magnetization loop with respect to the probing area. However, in the case of our sample, the defect did not significantly affect the magnetization loop, which is due to the fact that the density of defects in our sample is not large enough to govern the magnetic property of the nanodot array. To gain a further insight on the effect of defects on the magnetic property in our sample, we have performed a micromagnetic simulation of magnetization reversal in patterned dot array with the topological information quantitatively determined from the AFM image of the dot array. This enables us to take into account the geometrical defects of the nanodot array. Indeed, these simulations show that the magnetization loop for the perfectly aligned nanodot array is similar to that for the experimentally fabricated nanodot array.

In summary, we have fabricated a 2D patterned magnetic Co/Pt multilayer by using CL via a RIE process. The shape and size of the 2D nanostructures were controlled by adjusting simple RIE conditions, including the etching time and the number of colloidal layers. Enhancement of the magnetic properties of the

(19) Martín, J. I.; Nogués, J.; Kai, L.; Vicent, J. L.; Schuller, I. K. *J. Magn. Magn. Mater.* **2003**, *256*, 449.

(20) Chou, S. Y.; Krauss, P. R.; Kong, L. *J. Appl. Phys.* **1996**, *29*, 6101.

(21) Gibson, G. A.; Schultz, S. *J. Appl. Phys.* **1993**, *73*, 4516.

(22) Costa-Krämer, J. L.; Martín, J. I.; Menéndez, J. L.; Cebollada, A.; Anguita, J. V.; Briones, F.; Vicent, J. L. *Appl. Phys. Lett.* **2000**, *76*, 3091.

(18) Jeon, I.-J.; Kang, D.-W.; Kim, D.-E.; Kim, D.-H.; Choe, S.-B.; Shin, S.-C. *Adv. Mater.* **2002**, *14*, 1116.

metal dot array was demonstrated. This nanostructure control technique using CL may be applicable in the nanofabrication of patterned media.

Acknowledgment. This work was supported by a grant (M102KN010001-02K1401-00212) from the Center for Nanoscale Mechatronics & Manufacturing of the 21st Century Frontier Research Program and by the

Korean Ministry of Science and Technology through the Creative Research Initiatives Project. We also acknowledge partial support from the National R&D Project for Nano Science and Technology, Brain Korea 21 program, and CUPS-ERC.

CM048688S